◆ Human Brain Mapping 35:4858–4875 (2014) ◆

Movement-Related Neuromagnetic Fields in Preschool Age Children

Douglas Cheyne,[1]* Cecilia Jobst,[1] Graciela Tesan,[2,3] Stephen Crain,[2,4] and Blake Johnson[2,3]

[1]*Program in Neurosciences and Mental Health, Hospital for Sick Children Research Institute, Toronto, Ontario, M5G1X8, Canada*
[2]*Australian Research Council Centre of Excellence in Cognition and Its Disorders, Macquarie University, New South Wales 2109, Australia*
[3]*Department of Cognitive Science, Macquarie University, New South Wales 2109, Australia*
[4]*Department of Linguistics, Macquarie University, New South Wales 2109, Australia*

Abstract: We examined sensorimotor brain activity associated with voluntary movements in preschool children using a customized pediatric magnetoencephalographic system. A videogame-like task was used to generate self-initiated right or left index finger movements in 17 healthy right-handed subjects (8 females, ages 3.2–4.8 years). We successfully identified spatiotemporal patterns of movement-related brain activity in 15/17 children using beamformer source analysis and surrogate MRI spatial normalization. Readiness fields in the contralateral sensorimotor cortex began ~0.5 s prior to movement onset (motor field, MF), followed by transient movement-evoked fields (MEFs), similar to that observed during self-paced movements in adults, but slightly delayed and with inverted source polarities. We also observed modulation of mu (8–12 Hz) and beta (15–30 Hz) oscillations in sensorimotor cortex with movement, but with different timing and a stronger frequency band coupling compared to that observed in adults. Adult-like high-frequency (70–80 Hz) gamma bursts were detected at movement onset. All children showed activation of the right superior temporal gyrus that was independent of the side of movement, a response that has not been reported in adults. These results provide new insights into the development of movement-related brain function, for an age group in which no previous data exist. The results show that children under 5 years of age have markedly different patterns of movement-related brain activity in comparison to older children and adults, and indicate that significant maturational changes occur in the sensorimotor system between the preschool years and later childhood. *Hum Brain Mapp 35:4858–4875, 2014.*

Additional Supporting Information may be found in the online version of this article.

Contract grant sponsor: Australian Research Council Linkage Infrastructure Equipment and Facilities; Contract grant number: LEO668421; Contract grant sponsor: Australian Research Council Linkage Project Grant; Contract grant number: LP0669471; Contract grant sponsor: Australian Research Council Centre of Excellence for Cognition and its Disorders; Contract grant number: CE110001021, www.ccd.edu.au; Contract grant sponsor: Natural Sciences and Engineering Research Council of Canada; Contract grant number: NSERC RGPIN 184018.

*Correspondence to: Dr. Douglas Cheyne, Program in Neurosciences and Mental Health, The Hospital for Sick Children Research Institute, 686 Bay St, Toronto, Ontario, Canada, M5G0A8. E-mail: douglas.cheyne@utoronto.ca

Received for publication 29 October 2013; Revised 14 March 2014; Accepted 18 March 2014.

DOI 10.1002/hbm.22518

Published online 3 April 2014 in Wiley Online Library (wileyonlinelibrary.com).

Key words: MEG; movement-related fields; development; beamformers; sensorimotor oscillations; mu rhythm

INTRODUCTION

Neuroimaging of movement-related brain activity can provide insight into the neural mechanisms that govern the planning, initiation, and control of human action. Magnetoencephalographic (MEG) recordings of movement-related brain activity, combined with advanced source analysis techniques, allow for both the anatomical localization of movement-related brain activity and the analysis of the precise time course of brain activity during motor planning or execution, as well as frequency specific increases and decreases in rhythmic brain activity during motor tasks. Recent studies using various brain imaging techniques, including MEG, have indicated that oscillatory changes, particularly in the beta and gamma band, may play an important functional role in human motor control [Cheyne, 2013; Engel and Fries, 2010; Jenkinson and Brown, 2011]. Similarly, analysis of the movement-locked average brain response reveals distinct patterns of pre- and post-movement changes in the primary motor areas, characterized by motor fields (MFs) and movement-evoked fields (MEFs) [Cheyne and Weinberg, 1989; Kristeva et al., 1991; Nagamine et al., 1996]—the magnetic equivalents of the readiness and motor potentials observed in the electroencephalogram (EEG)—which reflect processes related to motor preparation and the processing of proprioceptive feedback important in both motor skills and learning.

However, to date there are relatively few neuroimaging studies of movement-related brain activity in early development. This is in part due to the technical challenges associated with neuroimaging studies in young children, including increased head and eye movement artifacts, and difficulty in getting young children to perform complex tasks. Functional MRI studies in very young children, in particular, are hampered by the low tolerance for even minute head movements and the intimidating environment of the MRI scanner. Even in the case of EEG, which is more readily adapted to studies in young children and infants [Tucker, 1993], there is a relative paucity of studies on movement-related brain activity in children younger than 6 or 7 years of age. The few studies to date have suggested that children show a very different scalp topography and polarity for the readiness potential compared to adults, with early pre-movement activity emerging only after the age of 6 years, but as an electrically positive potential, only developing into the negative readiness potential, or *Bereitschaftspotential* [Kornhuber and Deecke, 1965] observed in adults or children after 9 or 10 years of age [Chiarenza et al., 1995; Chisholm and Karrer, 1988]. There are also relatively few studies of movement-related rhythmic brain activity in children, although EEG studies in infants have demonstrated modulation of the mu rhythm during movement as early as 3 months of age [Berchicci et al., 2011; Marshall et al., 2011; Southgate et al., 2009].

In the case of MEG, a major obstacle for developmental studies is the fixed size of the helmet-shaped sensor array, which is designed to accommodate adult-sized heads. Nonetheless, MEG may have advantages over other imaging modalities for studies in young children; avoiding application of scalp electrodes reduces setup times and subject noncompliance, the MEG recording environment is quieter and less intimidating than an MRI scanner, and unlike fMRI, small amounts of head movement can be tolerated and in some cases even measured and corrected for [Wehner et al., 2008]. Still, there are relatively few MEG studies of motor development, and these have shown both similarities and differences to adult patterns in children that ranged in age from 5 or 6 years up to early adolescence [Gaetz et al., 2010; Huo et al., 2011; Wilson et al., 2010].

The sensorimotor cortex matures more rapidly than other brain areas [Giedd et al., 1999; Huttenlocher 1979] and conduction times of the descending corticospinal tract reaches adult values by 2 years of age, as shown by transcranial magnetic stimulation (TMS) of the motor cortex [Muller et al., 1991; Nezu et al., 1997]. However, these studies also demonstrate elevated stimulation thresholds, as well increased contributions of ipsilateral (uncrossed) descending pathways that persist up to early adolescence. Most notably, EMG "silent periods" ipsilateral to the side of stimulation, thought to reflect transcallosal inhibition of the opposite motor cortex, do not appear until after 6 years of age [Heinen et al., 1998]. This interhemispheric inhibition (IHI) may play an important role in the development of unilateral motor control, and account for bilateral motor cortex activity during unilateral movements in adults [Cheyne, 2008]. The gradual disappearance of mirror movement over the first decade of life [Mayston et al., 1999] and its persistence following early brain injuries [Rajapakse and Kirton, 2013] suggest that these inhibitory connections mature slowly, resulting in organizational changes within the motor system that continue throughout early childhood. Direct measures of such changes would increase our understanding of how typical patterns of motor control develop, as well as provide normative data for imaging studies involving cognitive-motor tasks in developmental populations.

To these ends, we carried out a study of movement-related brain activity in children 3 to 5 years of age using an MEG system customized for preschool children [Johnson et al., 2010]. We employed a novel videogame-like task designed to produce movements that were more self-

initiated, rather than responses to a visual or auditory cue. This task also proved engaging for the children, and avoided the problem of consistency in response timing or accuracy that can be problematic in very young children performing cued response tasks, and importantly, allowed us to observe motor preparatory activity (i.e., readiness fields) without significant overlap with evoked sensory responses. Source analysis was carried out using beamformer-based methods, which we have previously used for mapping motor responses in both adults and older children [Cheyne et al., 2007; Cheyne, 2013; Gaetz et al., 2010]. These methods reduce distortions in the reconstructed source images and their time courses due to eye blinks and eye movements [Bardouille et al., 2006; Cheyne et al., 2006; Herdman and Ryan, 2007] and other magnetic artifacts [Litvak et al., 2010] eliminating the need to discard large numbers of trials containing such artifacts, which can be problematic in children. We also had children perform the task with both their dominant and non-dominant hand, since little is known about the lateralization of these activity patterns in young children and their relationship to handedness. Finally, since MRI scans could not be obtained in these younger children, we used a surrogate MRI warping procedure for the purpose of source modeling, group averaging, and anatomical verification of source locations.

MATERIALS AND METHODS

Subjects

Seventeen healthy right-handed children (8 females, mean age 4.26 ± 0.13 years, range 3.2–4.9) participated in this experiment. Participants were recruited from the Sydney area and provided informed consent using protocols approved by the Macquarie University Human Subjects Ethics Committee. All children were assessed as being primarily right-handed using a modified version of the Edinburgh handedness inventory [Oldfield, 1971] for younger children. Children were asked to perform different actions with one hand: hammering, writing their name or drawing a picture, opening a jar, putting crayons into a box, throwing a ball, and cutting a piece of paper with child-safe scissors. The test was performed twice in separate sessions (introductory session and data collection session) for confirmation. Data from two children were excluded from the final analysis due to poor task compliance or excessively noisy data.

Stimulus and Task

The task and experimental setup (shown in Fig. 1A) consisted of a videogame-like task in which the children watched a computer display. In one version of the game children watched for the appearance of images of "aliens" intermixed with images of galaxies and satellites. Alien images appeared at the top of the screen at every 3 s and descended slowly toward the static image of a space ship image at the bottom of the screen. A 3-s inter-stimulus interval was found to provide sufficient baseline activity between movements without the children becoming bored or distracted during the task. The children were instructed to press a button with their index finger to launch a cookie toward the alien ("to feed the aliens") from a space ship. Motor responses were measured using a non-magnetic fiber optic response pad (LUMItouch Response System, Lightwave Medical Industries, Burnaby, Canada) held in both hands and resting on their body. Children were instructed to keep as still as possible and to press the button only once at a time but were allowed to maintain their own timing (i.e., they were not encouraged to respond quickly or as soon as the objects appeared). The task lasted 5 min in order to collect approximately 100 trials then repeated with the opposite hand (hand order counterbalanced across subjects). To help keep the children engaged in the task, explosive sounds were heard when the cookie reached the target; however, these were not time-locked to the appearance of the stimulus or the button-press.

A second version of the game utilized a fairytale theme: the spaceship and cookie images were replaced with forest characters (woodland animals, flowers, mushrooms) and a fairy character firing "magic dust." All other aspects of the two tasks in terms of number of items and timing were identical. Children were given a choice of which game they found most appealing and engaging. For the final analysis, data from the space-theme task was used for nine children, and data from the fairytale task for six children. The visual stimuli were presented on a back projection screen approximately 140 cm above the subject using an InFocus LCD projector (Model IN5108). Auditory feedback was presented via plastic tubes with insert earphones (Etymotic Research Inc., Model E-30, Elk Grove Village, IL).

Data Acquisition

Brain responses were measured using a whole-head MEG child system customized for measurements in preschool age children (Model PQ1064R- N2m, KIT, Kanazawa, Japan) in a magnetically shielded room (MSR) (Fujihara Co. Ltd., Tokyo, Japan) located at Macquarie University. This system consists of 64 first-order axial gradiometers with a 50 mm baseline in a helmet shaped array designed to fit approximately 90% of heads of 5-year old children. Further details of the MEG system specifications can be found in the work by Johnson et al. [2010] and Tesan et al. [2010]. All measurements were carried out with subjects in a supine position. An experimenter remained in the shielded room seated next to the children during the entire recording session. MEG data were acquired with a sampling rate of 1,000 Hz and filtered from 0.03 to 200 Hz. Head position was determined from

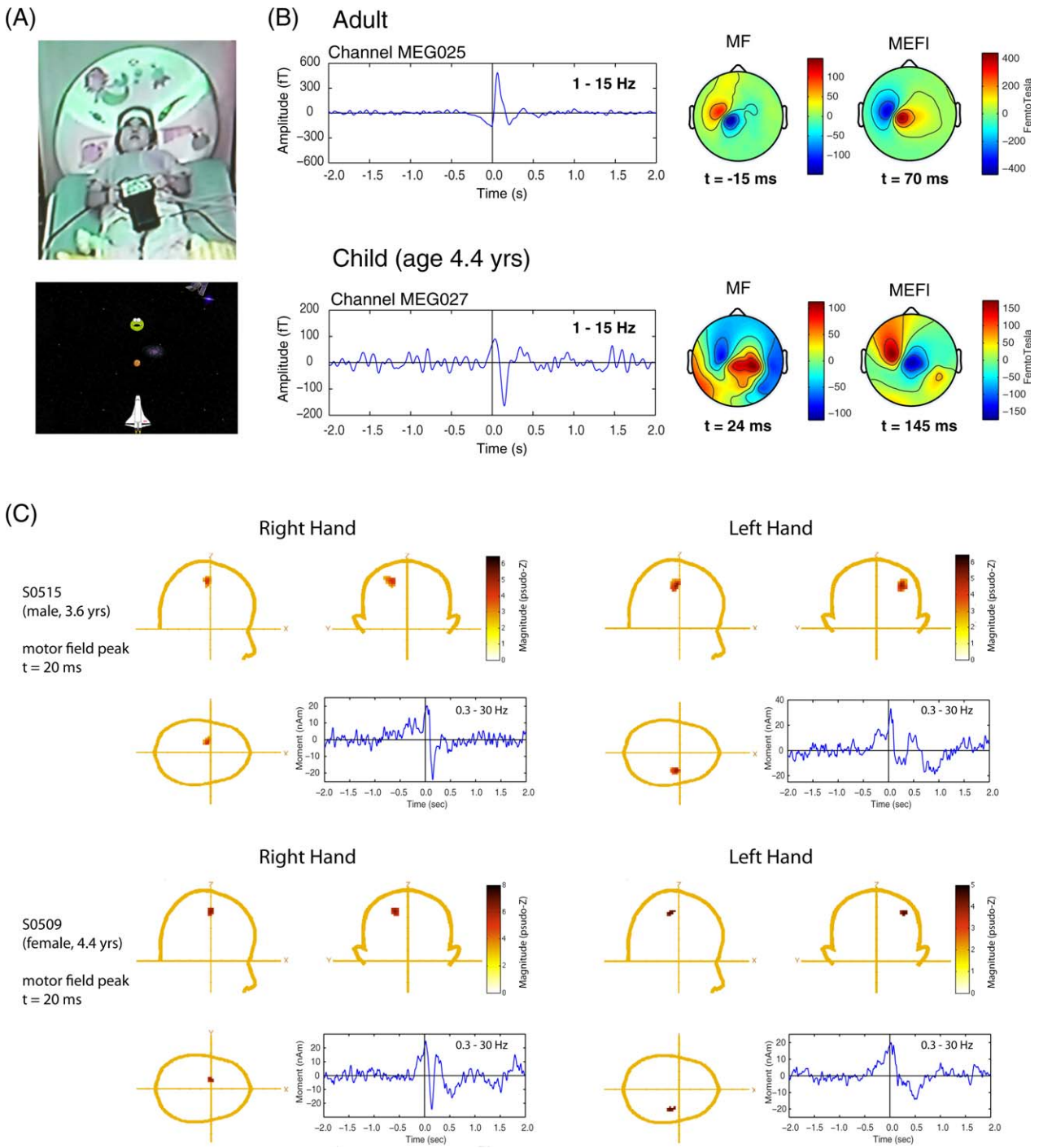

Figure 1.

A: Photograph of 4.8-year-old girl positioned in the Yokagawa child MEG system holding the Lumitouch response pad while viewing the visual display located on the MSR ceiling. A screen image of the space-game is shown below. **B**: Comparison of an averaged movement-related field (filtered 1–15 Hz) timelocked to the button press for a sensor overlying the left sensorimotor cortex from an adult subject (recorded in a 160 channel MEG system) and a 4.4-year-old boy recorded in the 60-channel child MEG system. Both systems were manufactured by KIT, Kanazawa, Japan and located side by side in the same magnetically shielded room. The field topographies of the MF and MEFI components are shown at the corresponding peak latency. Positive values indicate magnetic flux exiting the head (red colors) and negative flux entering the head (blue colors). Note the reversed field orientation and slight delayed latency of these components in the child. **C**: Examples of ERB analysis in two children for left hand versus right hand responses. The cartoon heads show the peak activity at the latency of the MF ($t = 20$ ms) and the corresponding time course filtered 0.3–30 Hz to show the slow readiness field beginning approximately 0.5 s prior to movement onset and transient MEFI component approximately 140 ms after movement onset. The latter is more distinct for the right (dominant) hand movements. [Color figure can be viewed in the online issue, which is available at wileyonlinelibrary.com.]

five head position indicator (HPI) coils secured to an elasticized cap placed on the child's head, tracked by the MEG system prior to and after each recording to determine total head movement. Recording sessions were terminated and repeated if head movement exceeded 5 mm or children stopped performing the task. The positions of the HPI coils and the subject's head shape were measured with a pen digitizer (Polhemus Fastrack, Colchester, VT) prior to the recording session, and the head shape data used to co-register the sensor positions with a head-based coordinate system based on fidicual locations located at the nasion and pre-auricular points.

Source Analysis

Localization of brain activity was carried out using both event-related and synthetic aperture magnetometry (SAM) beamformer algorithms, implemented in C++ and Matlab (Mathworks, Natick, MA) using the *BrainWave* toolbox developed at the Hospital for Sick Children (http://cheynelab.utoronto.ca). This includes an import module that converted the exported Yokogawa/KIT data files to a compatible data format, and transformed the MEG sensor geometry to the CTF head coordinate system, based on the location of the digitized fiducial coil placements relative to the sensor array. The raw data was segmented into 4-s epochs, from 2 s preceding to 2 s following each button press. Epochs were first extracted with additional data points (equal to 1/2 of the epoch length) at the beginning and end of each epoch window, and pre-filtered from 0.3 to 100 Hz using a bidirectional zero phase-shift Butterworth filter, then truncated to the 4 s time window to exclude end effects of the high-pass filter.

Head modeling and surrogate MRIs

For practical reasons it was not possible to obtain structural MRI scans in children for the purpose of head model determination, or normalization of images to a standard template for group averaging. To overcome this limitation, we used a "surrogate" MRI approach. First, we warped a template brain to each subject's digitized head shape using the iterative closest point algorithm implemented in SPM8 [Litvak et al., 2011] and the template scalp surface extracted with the FSL toolbox [Jenkinson et al., 2012]. This surrogate MRI was then used to fit a single-sphere conductor model [Sarvas, 1987] to the inner skull surface for source modeling [Lalancette et al., 2011], and to normalize source images to the standard MNI (T1) template brain, using both non-linear and linear spatial normalization implemented in SPM8 (Welcome Institute of Cognitive Neurology, London, UK). Source locations identified in MNI space were scaled to Talairach coordinates using the MNI to Talairach (mni2tal) conversion script [Brett et al., 2001] and compared to the Talairach atlas (www.talairach.org) for anatomical labeling [Lancaster et al., 2000]. This allowed us to average source images across children and perform non-parametric permutation tests [Singh et al., 2003] in order to assess the statistical reliability of source peaks, and determine their approximate anatomical locations.

The accuracy of the surrogate procedure was verified by comparing anatomical labeling in several adult subjects using a surrogate warped MRI and the subject's MRI, which resulted in good correspondence between both methods (e.g., motor activations localized to almost the identical brain locations using either method). We also tested the use of both a standard adult template, the Colin 27 (CH2) MRI [Holmes et al., 1998], and pediatric template brains available from the NIHPD database [Almli et al., 2007; Fonov et al., 2011] for surrogate warping in children, with the assumption that the latter would produce better approximation of the template brain structure to the child's brain anatomy due to better alignment in terms of skull thickness and brain morphology. We found that both templates produced very similar results in terms of anatomical labels, but that the pediatric template produced generally more consistent warping results with fewer failures (e.g., distorted looking surrogate MRIs). For the subsequent analysis, we used the 4.5–8.5 year old (asymmetric) pediatric template for surrogate warping. However, it should be noted that independently of which template is used, anatomical labeling from this procedure is still approximate, since it is dependent on the quality of the digitized head surfaces and how well the surrogate MRI matches each subject's true anatomy.

Event-related analysis

Event-related beamformer (ERB) analysis [Cheyne et al., 2006, 2007] was used to image averaged brain responses from MEG recordings time-locked to movement onset (button press). A time window from 1 s preceding to 0.5 s following movement onset was used to compute the data covariance for beamformer weight calculations using a bandpass of 1–30 Hz (to exclude low frequency and 50 Hz line noise that may affect localization accuracy). ERB images were volumetrically reconstructed using a 4 mm resolution grid covering the entire brain, at time points every 5 ms from 300 ms preceding to 300 ms following movement onset and inspected for peak locations of activity.

Since some subjects exhibited noisy images with multiple peaks of activity in the beamformer images, the following approach was used to identify MF peak locations in individual subjects. First, an experienced analyst identified peaks corresponding to the regions of contralateral motor cortex. The time-course of source activity was then computed as the output of the beamformer with optimized orientation ("virtual sensor") and plotted to identify the peak latencies of activity around movement onset, and this was compared back to peak activation in the volumetric images. Through this iterative approach it was possible to identify peaks of activation in almost all subjects, although

these were not always the largest peaks in the image. For example, in cases where two peaks were observed (e.g., as was the case of large activations in the right temporal region observed around movement onset), the peak corresponding to the sensorimotor area in the group image was taken as the motor cortex peak for that individual, even if it was smaller in amplitude. Group average time courses were then plotted to verify the latencies of peak activation around movement onset and revealed clear MF and MEFI-like amplitude peaks.

As a confirmatory analysis, group images in normalized (MNI) space were created for latencies of interest using the surrogate MRIs. An omnibus non-parametric permutation test was used to verify statistical significance of the group peaks. Locations of individual peaks were then obtained using an unwarping procedure (implemented in the *BrainWave* toolbox) whereby the peak MNI coordinate is transformed back into each individual subject's image and this location used as a seed to find the closest peak in the original source image within a fixed search radius (10 mm), in order to ensure that the true peak location was selected without relying on visual identification of peaks in the individual images. In the case where no larger peak within the search radius is found, the algorithm uses the original seed location. Comparison of peaks obtained from both analysis methods revealed similar localization results. Thus, for subsequent voxel-wise analyses, we used the locations and optimized orientations from the unwarping procedure.

Movement-related ERD and ERS

In order to examine induced rhythmic changes or event-related desynchronization or synchronization (ERD and ERS), we used the SAM algorithm [Robinson and Vrba, 1999]. Again, a two-step approach was used to establish source locations for oscillatory activity. First, time-frequency plots were created using the MF peaks identified in the ERB analysis to detect the timing and frequency of ERD and ERS events around movement onset. Time-frequency representations (TFRs) were then constructed using a Morlet-wavelet frequency transformation [Tallon-Baudry et al., 1997] of the 4-s single trial epochs of source activity and truncated to a time window of 1.5 s preceding, to 1.5 s following movement onset to exclude end effects of the wavelet transform. These were converted to percent change in power relative to a pre-movement baseline from -1.5 to -1 s to avoid overlap with the previous movement. This was confirmed by the observation of flat baseline activity in both the TFR plot and the averaged MFs up to 1.5 s prior to movement onset. In order to exclude power changes at lower frequencies that may be due to transient evoked fields accompanying movement onset, the mean power was subtracted from the single trial power to reveal only the non-phase-locked (*induced*) power changes [Makeig et al., 2004]. Time-frequency plots were averaged across subjects, and bootstrap resampling of the time-frequency reconstructions of all individual subject data (2,000 re-samplings of one-half of the images, with replacement) was used to estimate the standard errors and confidence intervals for peak gamma frequency and latency across individuals.

The second step involved computing whole-brain images of changes in narrow-band source power using SAM imaging [Robinson and Vrba, 1999] based on the power changes observed in the time-frequency plots. Pseudo-T difference images were created by subtracting the source power during an active time window of 500 ms duration from a baseline period of equal duration in mu (8–12 Hz), and beta (15–30 Hz) and high-gamma (60–90 Hz) frequency bands. This method has been used to successfully identify movement-related beta and gamma ERD and ERS in adults [Cheyne et al., 2008; Jurkiewicz et al., 2006]. Since the timing of ERD and ERS in the children was unknown, for the SAM analysis, the baseline power was computed from a time window from -1.0 to -0.5 s preceding movement onset and the active time window shifted in 50 ms increments from the period immediately following the control window to the period following the motor response. Time frequency analysis was then repeated with the peaks corresponding to the pseudo-T images. Group averaging and permutation thresholds were applied in the same manner as described for the event-related analyses to detect peak locations of oscillatory changes. Since we did not always observe clear peaks in the SAM pseudo-T images for individual subjects (this mostly occurred for weaker activations in the gamma band images but also for beta rebound), we used the ERB MFs peak locations and recomputed the beamformer weights with optimized source orientation to obtain the virtual sensor time series for time-frequency analyses.

RESULTS

Motor Fields and Movement-Evoked Fields

We observed movement-related field activity overlying the sensorimotor regions in all children. In some cases, the sensor level data was relatively noisy, presumably due to eye-movements and larger low frequency background variations than typically observed in adult subjects, although this varied across children and did not appear to be reflective of age (i.e., some of the youngest subjects produced the cleanest data). Averages of the sensor data and topographical plots for various latencies resembled that of adults with some key differences. These are illustrated in Figure 1B which compares the right finger movement data from a 4 1/2 year-old boy, and an adult subject performing a self-paced button press, measured with the 160-channel adult MEG Yokogawa system located in the same MSR, who shows the typical MF/MEFI pattern reported in the literature.

In the child subject, a slow pre-movement shift can be seen peaking around movement onset, indicative of the typical readiness field and MF in adults; however, the

latency of the MF peak was slightly delayed compared to the adult (15–25 ms after button press in comparison to −15 ms in the adult), and more importantly, shows a reversed topography, with a posterior directed source orientation (i.e., intracellular currents flowing in an anterior to posterior direction) for the MF, whereas the adult subject shows a typical anterior directed source pattern. This reversed polarity and delayed latency was also observed for the second component occurring at 130–140 ms after movement onset, which we assumed to be the equivalent of the MEFI in the adult, but with an anterior as opposed to posterior directed source orientation for the adult MEFI, which had a peak latency of 70 ms in the subject shown in Figure 1B.

To further confirm these observations at the sensor level, single dipole fits to the MF and MEFI field patterns were also carried out using the CTF DipoleFit program, which confirmed both a sensorimotor location and flipped orientation of the sources. Finally, to test for possible polarity flips due to the data export and conversion routines for the child MEG system, an adult female who could fit into the child system also performed the task and was found to produce similar (adult-like) latencies and MF/MEFI topographies in both systems. We also observed a field reversal overlying the temporal regions of the right hemisphere following movement onset, and this was present for both left and right finger movement conditions.

Beamformer Source Analysis

Event-related beamformer analysis confirmed sources in similar locations for both the MF and MEF in the region of the contralateral motor cortex in all children. Source images are shown for two individual subjects in Figure 1C, with clear contralateral MF peaks at 20 ms following movement onset (button press). Peaks are shown in MEG coordinates in the CTF head coordinate system as defined in the CTF MEG4 Software (MISL, Coquitlam, BC, Canada) and are therefore directly comparable to source coordinates from previous adult studies using the CTF system [e.g., Cheyne et al., 2006]. Source waveforms (virtual sensors) corresponding to the MF peaks are also shown using the same peak locations but with a high-pass filter setting of 0.3 Hz to reveal the slower readiness field, which can be seen to begin around 0.5 s prior to movement onset. It can also been seen that right index finger movements produced a sharper and more distinct MEFI peak in comparison to left finger movements in both subjects. Figure 2 shows MF peak locations for all subjects for left and right finger movements in the MEG coordinate system.

In general, the MEG coordinates of MF peaks were quite comparable in location to those reported in the literature in adults using the same fiducial-based coordinate system, although the peak scatter is relatively large, and locations in some subjects (but not all) slightly more medial in comparison to the typical adult coordinates. Source location variability was somewhat larger in the right hemisphere, possibly due to additional source activity in the right temporal lobe for all movements. Individual subject source locations for the MF in MEG coordinates, along with latencies of the MF, mean, and SE are provided in Table I. The mean latency of the MF was 18.0± 2.6 ms for right index button presses, and 18.3 ± 3.1 ms for left button presses. The MEFI peak locations varied slightly from those of the MF in individual subjects; however, these differences were not statistically significant across the group. MEFI latencies were 143.9 ± 10.7 and 131.1 ± 2.1 ms for right and left button presses, respectively. MEFI source parameters are provided in Supporting Information Table S1.

For group images corresponding to the peak amplitude of the MF at 20 ms, an omnibus permutation test indicated significant peaks in the (contralateral) left motor cortex for right index button presses (MNI coordinates: −20, −28, 54, $P < 0.001$) and in the right motor cortex for left button presses (MNI coordinates: 34, −20, 54, $P < 0.01$). After conversion to Talaiarach coordinates, both peaks corresponded to locations in precentral gyrus, BA4. Figure 3A shows the locations of the MF peaks superimposed on the CH2 template brain using the MRIcron [Rorden and Brett, 2000] program and the corresponding grand averaged source waveforms filtered from 0.3 to 30 Hz. Waveforms were highly similar for both left and right movements but with significantly smaller amplitude of the MF and MEFI peaks for left finger movements compared to right finger movements ($P < 0.05$). No significant correlation was found between MF amplitude or MF latency and age. Source parameters for the MF are shown for individual subjects in Table I. For the left button press a significant peak was also observed in the right superior temporal cortex at this latency corresponding to the right temporal lobe activation although the latter was not maximal at this latency (described in more detail below).

Oscillatory Brain Activity Accompanying Movements

We observed a suppression of beta band (15–30 Hz) activity prior to movement onset in all children. Group averaged time–frequency plots are shown in Figure 3B, showing beta suppression (ERD) (blue colors) beginning ∼200 ms prior to movement onset, transitioning to an ERS or "beta rebound" (red colors) between 500 and 1,000 ms, which lasted approximately 500 ms, although the termination of beta rebound in this case may have overlapped with preparatory activity related to the subsequent movements given a 3 s inter-movement interval. There was a noticeable delay between the offset of beta ERD and onset of rebound. This pattern and timing was consistent for both left and right hand movements. The mean frequency of beta suppression and rebound using bootstrap resampling across subjects was 18.08 ± 0.27 Hz (suppression) and 18.28 ± 0.45 Hz (rebound) for right index button

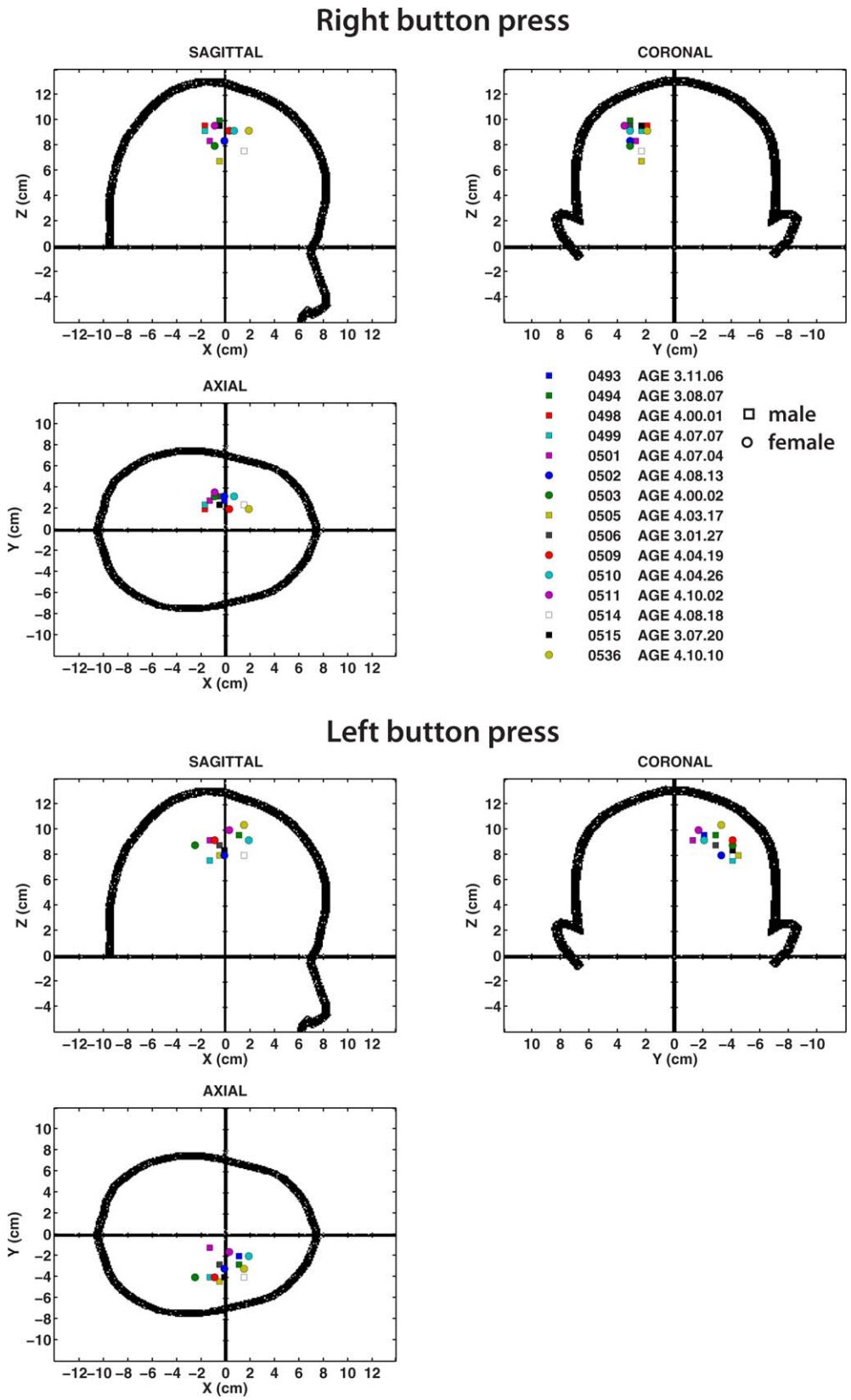

Figure 2.

Source locations of the MF in individual subjects, shown in the MEG coordinate system for right button presses (top) and left button presses (bottom). Coordinate system corresponds to the CTF MEG coordinate system which is a right-handed coordinate system with the +ve *x*-axis toward the nose and +ve *y*-axis toward the left ear. Locations for male subjects are shown as square symbols and for female subjects as circles. Note tighter clustering of sources for right compared to left button presses. [Color figure can be viewed in the online issue, which is available at wileyonlinelibrary.com.]

TABLE I. Motor field source parameters

Subject	Age (Y.M.D)	Sex	Latency (ms)	MEG coordinates (cm)			Talairach coordinates (mm)			Magnitude (pseudo-Z)	Brain location
				X	*Y*	*Z*	*X*	*Y*	*Z*		
Left button press											
0493	3.11.6	M	20	0.8	−2.0	9.6	26	−13	50	2.81	R Precentral Gyrus BA 6
0494	3.8.7	M	15	0.8	−3.6	9.2	38	−17	51	2.39	R Precentral Gyrus, BA 4
0498	4.0.1	M	20	−1.2	−4.0	9.2	46	−36	48	5.55	R Inferior Parietal Lobe, BA 40
0499	4.7.7	M	10	−1.2	−2.4	8.8	26	−36	48	4.18	R Postcentral Gyrus, BA 3
0501	4.7.4	M	25	−1.6	−1.6	8.8	26	−36	48	2.64	R Postcentral Gyrus, BA 3
0502	4.8.13	F	15	0.0	−3.2	8.0	34	−21	47	3.34	R Postcentral Gyrus, BA 3
0503	4.0.2	F	20	−0.4	−2.0	7.6	26	−22	36	3.08	R Cingulate Gyrus, BA 24
0505	4.3.17	M	10	−0.4	−4.4	8.0	50	−25	44	2.54	R Postcentral Gyrus, BA 2
0506	3.1.27	M	25	−0.4	−2.8	8.8	34	−25	40	2.17	R Postcentral Gyrus, BA 2
0509	4.4.19	F	0	−1.6	−4.0	8.8	42	−41	44	5.36	R Inferior Parietal Lobe, BA 40
0510	4.4.26	F	30	1.2	−2.4	9.2	34	−13	50	4.88	R Precentral Gyrus, BA 4
0511	4.10.2	F	20	0.4	−1.6	10.0	26	−17	54	5.31	R Precentral Gyrus BA 6
0514	4.8.18	M	25	1.6	−4.0	8.0	50	−2	39	3.54	R Precentral Gyrus BA 6
0515	3.7.20	M	45	−0.4	−4.0	8.4	42	−25	44	5.68	R Postcentral Gyrus, BA 2
0536	4.10.10	F	−5	1.2	−3.2	10.4	34	−13	54	3.17	R Precentral Gyrus BA 4
Mean			*18.3*	*−0.1*	*−3.0*	*8.9*	*35.6*	*−22.8*	*46.5*	*3.8*	
S.E.			*3.1*	*0.3*	*0.2*	*0.2*	*2.3*	*2.8*	*1.4*	*0.3*	
Right button press											
0493	3.11.6	M	0	−0.4	3.2	8.4	−34	−22	36	3.82	L Postcentral Gyrus, BA 3
0494	3.8.7	M	15	−1.2	2.8	9.2	−34	−25	47	3.76	L Precentral Gyrus BA 3
0498	4.0.1	M	20	−1.6	2.0	9.6	−22	−36	55	2.35	L Sub-Gyral, BA 40
0499	4.7.7	M	20	−2.0	2.4	8.8	−0	−44	48	3.51	L Superior Parietal Lobe BA 7
0501	4.7.4	M	0	−1.6	2.8	8.4	−22	−33	44	6.07	L Sub-Gyral, BA 31
0502	4.8.13	F	15	−0.4	3.2	8.0	−34	−25	47	4.81	L Precentral Gyrus BA 3
0503	4.0.2	F	10	−1.2	3.2	8.0	−34	−29	40	4.96	L Inferior Parietal Lobe, BA 40
0505	4.3.17	M	20	−0.8	2.8	6.8	−26	−22	29	3.17	L Sub-Gyral
0506	3.1.27	M	15	−0.8	3.2	10.0	−34	−29	51	4.13	L Postcentral Gyrus, BA 3
0509	4.4.19	F	25	0.0	2.0	9.2	−26	−25	51	6.12	L Precentral Gyrus, BA 4
0510	4.4.26	F	25	0.4	3.2	8.8	−34	−17	47	5.94	L Precentral Gyrus, BA 4
0511	4.10.2	F	20	−1.2	3.6	9.6	−38	−33	48	5.85	L Inferior Parietal Lobe, BA 40
0514	4.8.18	M	20	1.2	2.4	7.2	−18	5	31	4.29	L Cingulate Gyrus, BA 32
0515	3.7.20	M	40	−0.8	2.4	9.2	−26	−24	55	5.54	L Precentral Gyrus BA 4
0536	4.10.10	F	25	1.6	2.4	9.6	−26	−9	47	7.97	L Middle Frontal Gyrus, BA 6
Mean			*18.0*	*−0.6*	*2.8*	*8.7*	*−29.2*	*−24.5*	*45.1*	*4.8*	
S.E.			*2.6*	*0.3*	*0.1*	*0.2*	*1.5*	*3.0*	*2.0*	*0.4*	

presses, and 18.29 ± 0.46 Hz (suppression) and 18.07 ± 0.30 Hz (rebound) for left button presses. We also observed a highly similar pattern of suppression and rebound in the mu band (8–12 Hz) with similar timing. Mean frequency of mu suppression and rebound was 9.03 ± 0.12 Hz (suppression) and 8.98 ± 0.09 Hz (rebound) for right index button presses, and 9.26 ± 0.16 Hz (suppression) and 8.93 ± 0.14 Hz (rebound) for left button presses. The relative locations of beta and mu suppression obtained from the SAM pseudo-T images indicated that the mu suppression was more bilateral (slightly weaker ipsilateral), whereas the beta suppression was strongly contralateral to the side of movement. As shown in Table II, both mu and beta band activity showed locations in similar regions of the postcentral gyrus, with no significant differences in anterior–posterior or lateral position, although locations were more inferior for beta band peaks for both left and right movements ($P < 0.01$, paired *t*-tests, corrected).

Movement-induced motor gamma synchronization was observed for source locations in the sensorimotor cortex and consisted of brief, narrow band oscillations of a few hundred milliseconds duration, similar to that reported in adults [Cheyne et al., 2008; Muthukumaraswamy, 2010]. Children demonstrated a robust high frequency gamma (70–80 Hz) burst at movement onset, similar to the adult form, or a low gamma (35–40 Hz) burst at the same latency, and some subjects showed equal amounts of both high and low gamma bursts. These three different patterns of movement-evoked gamma oscillations in the sensorimotor cortex are shown in three selected subjects in Figure

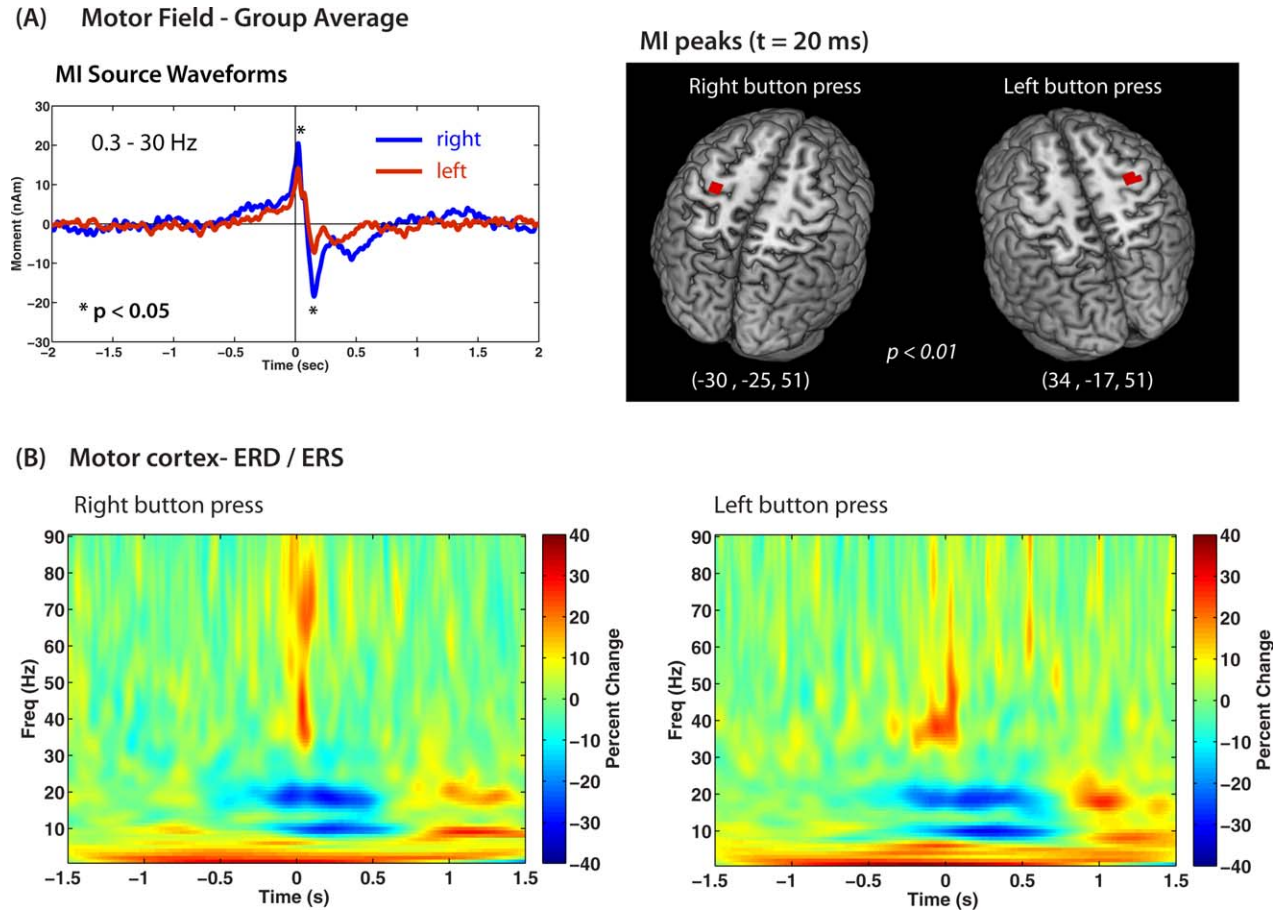

Figure 3.

A: Group averaged ERB source waveforms for all 15 subjects shown for right button press (blue trace) and left button press (red trace) conditions. Bandpass 0.3–30 Hz. Amplitude of the MF and MEFI components (asterisks) was significantly greater for right compared to left movements (asterisks). The peak locations of the MF for both movement conditions is shown superimposed on the MNI template brain, thresholded at the $P < 0.01$ level using surrogate MRI warping. Talairach coordinates for each peak are shown and correspond to locations near the hand area of the pre-central gyrus. **B**: Time-frequency plots of the group averaged induced power changes (averaged power subtracted) with increases (red) and decreases (blue) around movement onset (button press = 0 s) showing mu and beta band modulations and low and high gamma bursts at movement onset. Note delayed onset of mu and beta suppression and rebound, and absence of high gamma activity for left movements. [Color figure can be viewed in the online issue, which is available at wileyonlinelibrary.com.]

4A. To better quantify these two different movement-related gamma activations, group time–frequency reconstructions were plotted across all subjects, using bootstrap resampling in two different frequency ranges; a "high gamma" 60–90 Hz frequency band and a "low gamma" frequency range of 30–60 Hz, shown in Figure 4B. (Time–frequency plots for individual subjects are provided in Supporting Information). Virtual sensors were recomputed with optimized orientation for each frequency band prior to time–frequency analysis, measured in percent change from baseline (−2 to −1 s) to correct for $1/f$ bias in the scaling of the plots. Peak frequency for the high (60–90 Hz) gamma band burst was 71.2 ± 3.1 Hz for right button presses and 75.5 ± 4.3 Hz for left button presses. For the low (30–60 Hz) gamma burst mean peak frequency was 38.7 ± 2.4 Hz for right button press and 46.3 ± 4.1 Hz for left button press.

Right Temporal Lobe Activation

In addition to activations in the sensorimotor cortex, we also observed highly significant ($P < 0.002$) movement-locked activity in the posterior region of the right temporal gyrus in both right and left button press conditions. Group images revealed almost identical locations in the right

TABLE II. Mu (8–12 Hz) and beta (15–30Hz) mean pseudo-T peak source parameters

	Contralateral Talairach coordinates (mm)			Magnitude (pseudo-Z)	Brain location	Ipsilateral Talairach coordinates (mm)			Magnitude (pseudo-Z)	Brain location
	X	*Y*	*Z*			*X*	*Y*	*Z*		
Left button press										
Mean mu	39	−23	44	−19.05	R Postcentral Gyrus, BA 2	−34	−26	46	−18.33	L Postcentral Gyrus, BA 3
S.E.	1.94	2.84	1.96	1.93		3.06	4.18	2.11	3.02	
Mean beta	39	−22	36	−6.35	R Postcentral Gyrus, BA 3	−40	−22	39	−5.18	L Postcentral Gyrus, BA 3
S.E.	1.89	2.54	2.62	0.81		5.00	2.40	3.76	0.52	
Right button press										
Mean mu	−36	−19	48	−12.81	R Precentral Gyrus, BA 4	40	−27	43	−12.41	L Postcentral Gyrus, BA 40
S.E.	3.00	4.31	3.05	1.65		4.62	3.39	4.70	1.67	
Mean beta	−33	−22	40	−6.62	R Postcentral Gyrus, BA 3	39	−24	40	−4.89	L Postcentral Gyrus, BA 2
S.E.	1.83	3.88	2.53	0.87		5.81	9.07	2.60	0.73	

superior temporal gyrus (close to the posterior insula) for left and right movements, as shown in Figure 5. Virtual sensor analysis of these peaks revealed that these sources also showed highly similar time courses, with a slow increase beginning prior to movement onset, reached peak amplitude at ∼70 ms after movement onset, followed by a slow shift of opposite polarity that reached maximal amplitude between 500 and 700 ms.

DISCUSSION

Very little is known about the early development of motor control in children, and the corresponding changes in sensorimotor regions of the brain. In a recent review of brain development and neuroimaging in preschool age children [Brown and Jernigan, 2012], the terms "*movement*" and "*motor cortex*" are completely absent, and only a few MEG studies of brain function are described, focusing primarily on language and sensory processing. Human motor skills mature relatively early in life, with many basic abilities present by the age of 8 years [Piek et al., 2012] suggesting that the typical patterns of movement related brain activity observed in adults should be present at a relatively early stage of development, yet such measures have not been carried out in children of preschool age or younger. In the current study, we were able to obtain recordings of self-initiated finger movements in a group of 3 to 5 year-olds using a custom MEG system designed for preschool age children. The self-paced nature of their movements was confirmed by the observation of pre-movement readiness fields that preceded the button press by up to several hundred milliseconds. Using beamformer source localization combined with surrogate MRI normalization, we were able to identify cortical sources of movement-locked MFs and induced oscillatory changes in the mu, beta, and gamma bands activity in all children. This allowed us to directly compare movement-related brain activity for simple, self-paced motor responses in preschool age children to that previously described in adults, as discussed in the following sections.

Movement-Related Magnetic Fields

Pre-movement MFs were observed in all children and their underlying generators localized to the contralateral precentral gyrus (Brodmann area 4) in agreement with source locations found in adults [Cheyne et al., 2006; Kristeva et al., 1991]. These results confirm that it is possible to localize motor cortex activation using MEG in preschool age children, and that the surrogate template normalization approach using digitized head shapes provides a reliable method for group averaging when structural MRI is unavailable. An unexpected finding, however, was that both the MF and MEFI were both delayed and reversed in topography (source orientation) compared to that reported for adults. For example, for self-paced finger movements in adults, the MF peaks around 50 ms prior to a mechanical button press, roughly coinciding with onset of EMG activity in the agonist muscles, followed the movement evoked field I (MEFI) around 100 ms later [Cheyne and Weinberg, 1989; Kristeva et al., 1991]. We observed a slowly increasing MF, of opposite polarity to adults, which reached peak amplitude around 18 ms after the button press, followed by a transient response resembling the MEFI 120–130 ms after the MF. The delayed MEFI latency might suggest that the children simply executed movements more slowly. Unfortunately, it was not possible to obtain EMG recordings in the current study to assess movement speed or duration. However, we used a highly

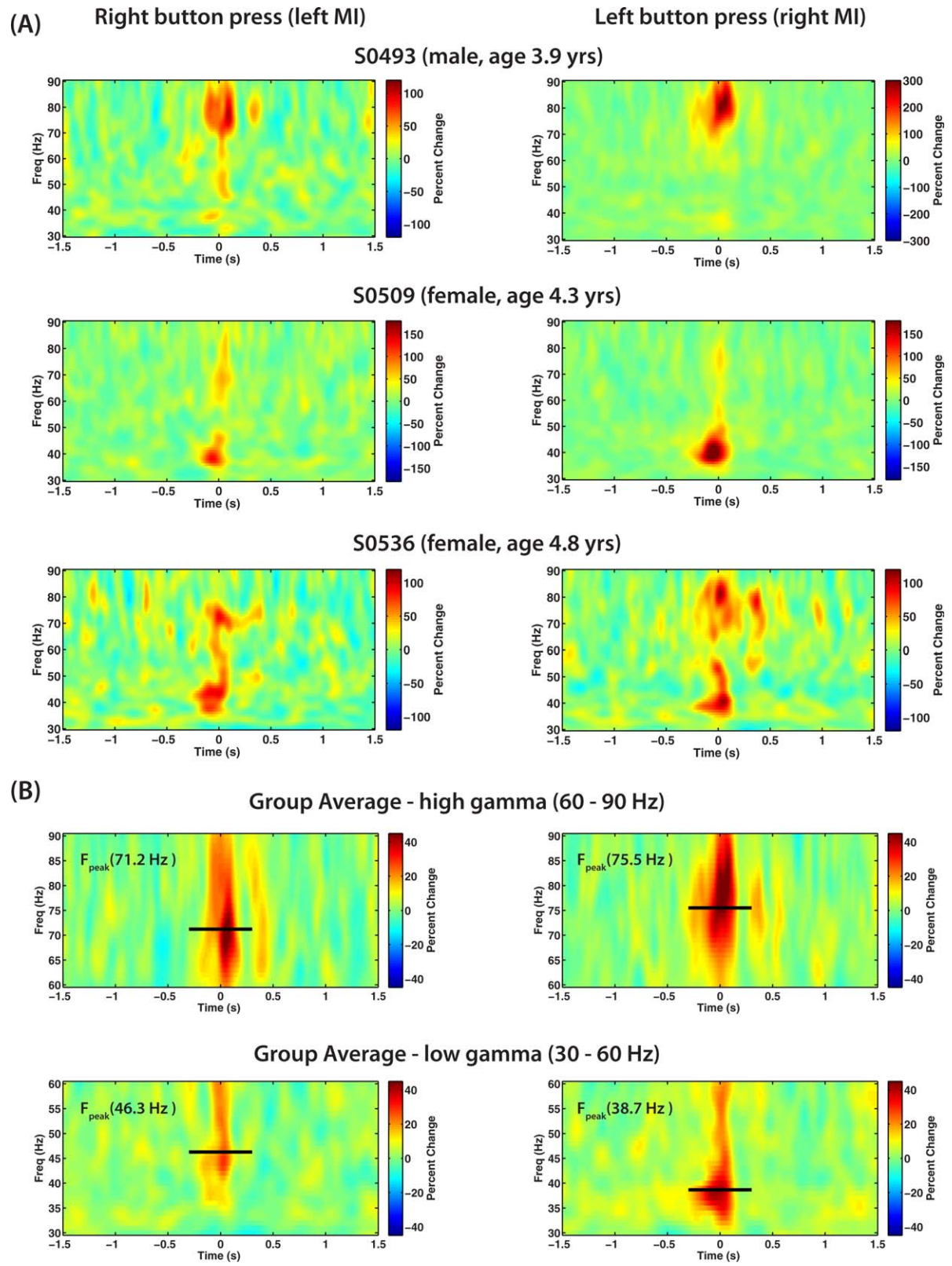

Figure 4.

A: Time–frequency plots of movement induced source activity in the gamma band (30–90 Hz) in contralateral motor cortex (MI) for left and right button presses in three different representative subjects that showed either only high frequency gamma activation around 80 Hz (first row), only low frequency gamma activation around 38 Hz (second row), or both high and low frequency gamma activation (third row) at movement onset ($t = 0$ s). **B**: Gamma band source activity in contralateral MI for both high gamma band (60–90 Hz) or low gamma range (30–60 Hz) averaged over all subjects. The black horizontal line and text (F_{peak}) shows the estimated peak frequency using bootstrap resampling of one-half of all subjects. The length of the line shows the time period over which peak frequency was estimated (−0.3 to 0.3 s). [Color figure can be viewed in the online issue, which is available at wileyonlinelibrary.com.]

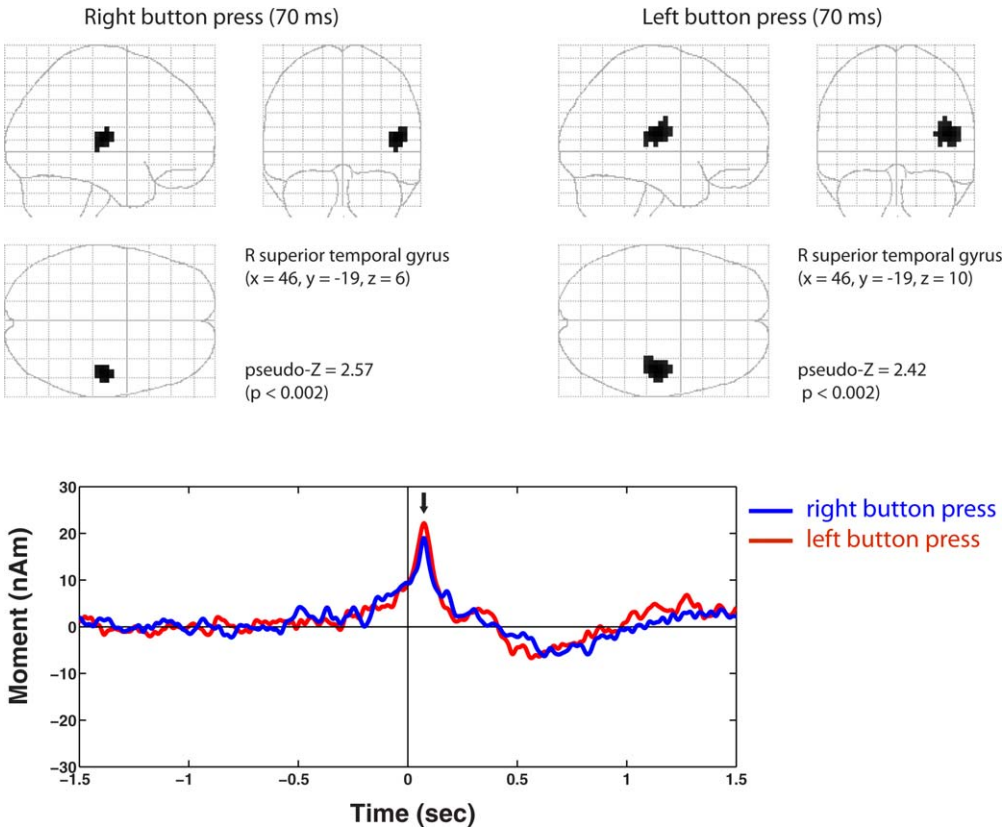

Figure 5.

Movement-locked activation of a source in the right temporal gyrus was observed for both left and right button press conditions with peak activation at ~70 ms. Source location shown in MNI coordinates, permutation threshold = $P < 0.002$. Note almost identical locations (shown in Talairach coordinates with corresponding atlas labels) for both conditions. These peaks showed remarkably similar time courses (shown below) peaking at latency of 70 ms (black arrow) with a slower activation around 0.5–0.7 s following movement onset. [Color figure can be viewed in the online issue, which is available at wileyonlinelibrary.com.]

sensitive response pad that triggered with minimal finger displacement, and children were not observed to make overtly slow movements (on the contrary they tended to perform the task quickly). Also, we would predict an earlier rather than delayed MF for slow movements, due to delayed triggering of the switch. The reversed polarity of the MF is consistent with a reported reversed polarity of the readiness potential in children younger than 6 years of age [Chiarenza et al., 1995] and suggests that there is a transition in terms of the underlying generators of the classic readiness potential observed in adults around this period of development, the physiological basis of which remains to be determined.

Differences in morphology and polarity of sensory evoked responses are observed in both neonates and young children. Most relevant to the current study, Pihko et al. have shown that the somatosensory evoked field (SEF) waveform undergoes many changes during early life, and does not resemble the adult form in even at 6 years of age [Pihko et al., 2009]. In particular, the posterior directed M50 component was absent in two-year old children, who showed instead a weaker peak of opposite polarity [Pihko et al., 2009, Fig. 7]. For the electrical SEF, the earliest components show the same source orientation as compared to a positive–negative reversal observed in adults [Lauronen et al., 2006]. Thus SEFs demonstrate large changes in both timing and polarity up to late childhood. One interpretation of such changes is that the polarity of the underlying generators remains constant and latency shifts (e.g., due to axon myelination) can mimic changes in polarity. However, we do not believe that this is the case for the reversed MF, as it demonstrated an early onset (about 1/2 s prior to movement) and a slow increase peaking at movement onset, very similar to that of the adult MF.

Similarly, the delayed and reversed MEFI might be interpreted as an MEFII, which shows a similar polarity and latency in adults [Kristeva et al., 1991]. This would imply a complete absence of the MEFI component at this age. In addition, MEFI source location was not

significantly posterior to the MF, as shown in a previous adult study [Cheyne et al., 2006] raising the possibility that both the MF and MEFI components described here arise from precentral structures (as shown also for the MEFII). The MEFI has been directly related to proprioceptive (muscle spindle) feedback during movement [Cheyne et al., 1997; Onishi et al., 2006]. Little is known about the early development of proprioceptive control of movement in children, although kinematic studies have shown that fingertip force control continues to improve throughout childhood with a marked increase in force stability after the age of 6 years [Dayanidhi et al., 2013; Forssberg et al., 1991]. Thus, some differences observed in post-movement responses during the button press task might reflect developmental changes in the processing of proprioceptive input to sensorimotor cortex during dexterous finger movements.

Differences in MF polarity are more difficult to interpret, but may be analogous to developmental changes observed for auditory evoked responses. The vertex-negative N100 response in children younger than about 12 years of age is dominated by a vertex positivity (the P100) and the N100 is thought to emerge gradually between adolescence and adulthood [Picton and Taylor, 2007], and this has been confirmed using MEG recordings in different age groups including preschool age children [Johnson et al., 2010, 2013]. One explanation is that the child P100 is the precursor of the adult P50 [Lippe et al., 2009], which gradually decreases in latency with age, while the surface negativity producing the N100 requires the formation of functioning synaptic connections in the dendritic branches of the upper layers of the auditory cortices [Moore and Guan, 2001; Ponton et al., 2000, 2002]. Others, however, suggest that the N100 is present in the child response but obscured by the larger amplitude and temporal overlap of the immature P50 response [Picton and Taylor, 2007]. The neural generator of the MF can be modeled as anterior directed (intracellular) currents in the precentral gyrus, consistent with apical depolarization of pyramidal cells in primary motor cortex (MI) generating the vertex negative readiness potential [Cheyne and Weinberg, 1989; Kristeva et al., 1991]. The absence of a negative readiness potential observed in younger children [Chiarenza et al., 1995; Chisholm and Karrer, 1988] might similarly indicate less excitatory input to superficial layers of MI. This could also be accompanied by a shift of activation to more anterior (or gyral) portions of the precentral gyrus during development that would produce a larger negative potential over the vertex and perhaps a flip in orientation of the magnetic fields. However, further longitudinal studies will be required to determine whether the patterns observed here undergo such polarity transitions with age to support this hypothesis.

Interestingly, MF and MEFI amplitude was significantly larger for right (dominant) hand movements compared to left-hand movements. Some also showed earlier MF onset for right hand movements, as has been previously reported in adults [Cheyne, 2008], as well as a more distinct MEFI peak. These differences might be attributed to less coordinated movements of the left (non-dominant) hand resulting in increased variability in timing and less synchronization of the evoked fields. However, there was also a greater presence of high-frequency gamma at movement onset for right compared to left hand movements (Fig. 3B), and the latter showed predominantly lower gamma bursts. Thus, patterns of movement-related brain activity appear to reflect hand dominance in children as young as 3 years of age. It has been suggested that increased readiness potential amplitude with age reflects a decreased need to suppress mirror movement [Chisholm and Karrer, 1988], and concomitant changes in interhemispheric inhibition associated lateralized motor control [Mayston et al., 1999]. In this regard, it is noteworthy that we did not observe highly bilateral motor cortex activity, even though one might predict greater mirror movements in the children (although these were not directly measured in the present study). This lends support to the hypothesis that ipsilateral readiness fields in adults are related to suppression of mirror movements during unilateral movements [Cheyne, 2008; Kristeva et al., 1991]. Further comparative studies in left-handed children or changes in mirror movements with age will be required to test these hypotheses further.

Finally, it should be noted that we did not observe early pre-movement activity in midline structures such as the supplementary motor area. Two possible reasons are the lower signal to noise ratio of the children's data, and the more rapid cued nature of the experimental task in the present study [Erdler et al., 2000].

Movement-Related Beta and Mu Rhythms

Self-paced movements in adults are accompanied by modulations of mu and beta band oscillations [Pfurtscheller and Aranibar, 1977; Pfurtscheller, et al., 1996]. These include the well-known suppression of mu and beta oscillations (ERD) that begin up to 1.5 s prior to movement onset and transitions to beta synchronization (ERS) within 1/2 s of movement offset [Cassim et al., 2001; Jurkiewicz et al., 2006]. Previous MEG studies have reported beta ERD and ERS in older children and adolescents with marked decreases in younger children [Gaetz et al., 2010; Huo et al., 2011; Wilson et al., 2010]. In the current study, we observed both mu and beta ERD in the children but with a later latency, around 200–250 ms prior to movement onset.

This later ERD onset might be attributed to our use of cued movements instead of the self-paced movement paradigm employed in the previous studies (the 3–5 year olds studied here did not have the capacity to generate self-paced movements in any reliable or consistent fashion). However, this interpretation is inconsistent with the fact that the onset of the MF was similar to self-paced

movements in adults. Beta rebound ERS was also present in the children, but began 200–300 ms after beta power returned to baseline, as opposed to the rapid transition seen in adults. As beta rebound is time-locked to movement offset [Alegre et al., 2002; Jurkiewicz et al., 2006] this might be attributed to longer or more variable movement duration in the children.

A notable observation was that frequency tuning of both mu and beta band ERD and ERS in the child data was much narrower than the rather broad frequency bands modulated by movement in adults. In the children, mu and beta oscillations appeared to be almost harmonically related, with mean frequencies of ~9 and 18 Hz, respectively. Mu and beta also followed very similar ERD/ERS time courses, although mu suppression began slightly later. In comparison, beta power changes in adults tends to be distributed over a broad frequency range extending from 15 Hz to 30 Hz or higher [Jurkiewicz, et al., 2006] and mu band suppression does not demonstrate a post-movement overshoot or rebound, but continues throughout the movement period. Thus, modulation of beta and mu rhythmic activity appears to be much more tightly coupled and lower in frequency in the immature sensorimotor cortices. A recent EEG study reported a rapid and linear increase in mu frequency from 2 to 8 Hz between 11 and 47 weeks of age, reaching a stable value of about 8.5 Hz between 2 and 4 years of age [Berchicci et al., 2011]. This is consistent with our observation of mu frequency at around 9 Hz in our subjects and indicates that mu frequency remains stable at lower frequencies until at least 5 or 6 years of age. Mu oscillations in adults are typically in the range of 10–13 Hz, indicating that there is a further increase in mu frequency during adolescence.

The neurogenesis of sensorimotor mu and beta rhythms is not fully understood. Jones et al. [2009, 2010] have proposed a model whereby both mu and beta oscillatory activity result from combined feedback and feedforward ≈ 10 Hz input from the thalamus to different layers of the somatosensory cortex—i.e., both beta and mu oscillations arise from subcortical drive in the mu frequency band. The strong correspondence between movement-related mu and beta oscillations in the immature brain might reflect such network coupling. In support of this interpretation, mu and beta oscillations in the children were localized to very similar postcentral locations (although slightly more inferior for beta) in contrast to studies showing postcentral locations of mu activity and precentral locations for beta oscillations in adults [Jurkiewicz et al., 2006; Salmelin and Hari, 1994]. This suggests that the mu and beta rhythms in younger children may arise from similar neural populations in somatosensory cortex. The prevalence of beta oscillations have also been associated with age-related changes in inhibitory neurotransmitter levels [Gaetz et al., 2010]. However, our results suggest that children younger than 6 years of age exhibit both different timing and relative amounts of mu and beta reactivity to movement, perhaps reflecting maturational differences within cortical-subcortical networks, such as increased proprioceptive feedback to MI, which may generate the more anterior sources of beta rebound observed in adults.

Movement Related Gamma Oscillations

All children exhibited movement-induced high-frequency gamma oscillations very similar in frequency and timing to that described in adults. These are narrowly-tuned high-frequency oscillations in the 70–80 Hz range observed in the contralateral motor cortex at movement onset [Cheyne et al., 2008]. These are observed only during active movements [Muthukumaraswamy, 2010] and are highly stable over time [Cheyne and Ferrari, 2013]. Importantly, similar gamma activity is observed in subcortical structures suggesting that they play an important role in cortico-subcortical motor circuits [Lalo et al., 2008]. The current study confirms that similar movement-induced gamma activity is observed in children as young as 3 years of age. However, some of the children exhibited narrow band oscillations with similar timing and duration, but at a much lower frequency range of 35–45 Hz, and some of the children showed both high and low frequency motor gamma bursts simultaneously.

It is interesting to speculate whether the presence of high and low gamma bursts in some of the children reflects a transition to the adult pattern around this age. Further longitudinal studies will be required to confirm this. However, taken together with the differences observed in the beta and mu band activity, the current findings suggest that there may be structural and functional changes in motor circuits during early childhood that impact the frequency "tuning" of oscillatory activity in cortical motor areas. These may be related to changes in connectivity between cortical areas (e.g., transcallosal inhibition) or subcortical (e.g., thalamocortical) structures, due to increased myelination in long-range pathways. It has also been speculated that the frequency of gamma oscillations increases with age due to changes in inhibitory (GABA) neurotransmitter levels [Gaetz et al., 2011; Muthukumaraswamy et al., 2009]; however, the youngest children in our study showed motor gamma activity at the same frequencies as that reported in adults.

Right Temporal Lobe Activation

Another unexpected observation was the activation of the posterior portion of the right superior temporal gyrus by both left and right hand movements. We note that the appearance of the target object (cookie or wand) was initiated by the subject and coincided with the button press. As the right temporo-parietal region is implicated in processing of visual motion, particularly biological motion [Grezes and Decety, 2001; Jokisch, et al., 2005], it is tempting to ascribe this activation to self-induced visual motion. This activity demonstrated a slow pre-movement onset, and reached peak amplitude at 70 ms, and is thus unlikely to be simply

a visual evoked response to motion onset. Interestingly, activation of this brain area is also observed in tasks involving anticipation of self-triggered visual motion and may be related to the so-called "when pathways" of the dorsal visual attention network [Battelli et al., 2007]. Alternatively, this may be a purely movement-related activation that is unique in this age group for precisely timed movements. We have observed pre-movement activity in the left parietal region for self-paced tasks in adults using similar analysis methods [Cheyne et al., 2006] indicating that parietal regions may also show time-locked MFs. Additional experiments using comparably cued movements will be required to determine whether this paradigm elicit similar responses in the adult brain.

CONCLUSIONS

The results of the current study provide novel data on sensorimotor brain function for an age-range in which there is currently a paucity of functional neuroimaging data and which has never previously been studied using MEG in a voluntary movement paradigm. These results provide new insights into the functional organization of the developing motor system. The timing and morphology of movement-related brain activity in the child brain shows that maturation of the motor system is incomplete in the preschool years and thus must undergo significant changes in organization in the next several years, when comparable brain responses have essentially adult properties. This establishes a new and previously unknown functional discontinuity over development that may have important implications for the study of motor development in both healthy and disordered populations. It is unknown when the transition between immature and adult-like neuromagnetic motor responses occurs. Our data narrow the possible time window to between ages 3 and 5 and about age 8, providing clear direction for subsequent longitudinal studies. This functional discontinuity also suggests that some caution is needed in selecting age ranges for functional neuroimaging studies in children performing tasks that involve motor responses. On a practical level, this study demonstrates that the use of a custom pediatric MEG system provides signal-to-noise levels that are adequate to localize MFs to the primary motor cortex in children as young as 3 years of age.

ACKNOWLEDGMENTS

The authors thank Wendy Tham for technical assistance and acknowledge the collaboration of Kanazawa Institute of Technology in establishing the KIT-Macquarie MEG laboratory.

REFERENCES

Alegre M, Labarga A, Gurtubay IG, Iriarte J, Malanda A, Artieda J (2002): Beta electroencephalograph changes during passive movements: Sensory afferences contribute to beta event-related desynchronization in humans. Neurosci Lett 331:29–32.

Almli CR, Rivkin MJ, McKinstry RC (2007): The NIH MRI study of normal brain development (Objective-2): Newborns, infants, toddlers, and preschoolers. NeuroImage 35:308–325.

Bardouille T, Picton TW, Ross B (2006): Correlates of eye blinking as determined by synthetic aperture magnetometry. Clin Neurophysiol 117:952–958.

Battelli L, Pascual-Leone A, Cavanagh P (2007): The 'when' pathway of the right parietal lobe. Trends Cogn Sci 11:204–210.

Berchicci M, Zhang T, Romero L, Peters A, Annett R, Teuscher U, Bertollo M, Okada Y, Stephen J, Comani S (2011): Development of mu rhythm in infants and preschool children. Dev Neurosci 33:130–143.

Brett M, Christoff K, Cusak R, Lancaster J (2001): Using the Talairach atlas with the MNI template. NeuroImage 13:S85.

Brown TT, Jernigan TL (2012): Brain development during the preschool years. Neuropsychol Rev 22:313–333.

Cassim F, Monica C, Szurhaj W, Bourriez J-L., Defebvre L, Derambure P, Guieu J-D. (2001): Does post-movement beta synchronization reflect an idling motor cortex? NeuroReport 17:3859–3863.

Cheyne D (2008): Imaging the neural control of voluntary movement using MEG. In: Fuchs A, Jirsa VK, editors. Coordination: Neural Behavioral and Social Dynamics. Berlin: Springer. pp 137–160.

Cheyne DO (2013): MEG studies of sensorimotor rhythms: A review. Exp Neurol 245:27–39.

Cheyne D, Weinberg H (1989): Neuromagnetic fields accompanying unilateral finger movements: Pre-movement and movement-evoked fields. Exp Brain Res 78:604–612.

Cheyne D, Ferrari P (2013): MEG studies of motor cortex gamma oscillations: Evidence for a gamma fingerprint in the brain? Front Hum Neurosci 7:575.

Cheyne D, Endo H, Takeda T, Weinberg H (1997): Sensory feedback contributes to early movement-evoked fields during voluntary finger movements in humans. Brain Res 771:196–202.

Cheyne D, Bakhtazad L, Gaetz W (2006): Spatiotemporal mapping of cortical activity accompanying voluntary movements using an event-related beamforming approach. Hum Brain Mapp 27:213–229.

Cheyne D, Bostan AC, Gaetz W, Pang EW (2007): Event-related beamforming: A robust method for presurgical functional mapping using MEG. Clin Neurophysiol 118:1691–1704.

Cheyne D, Bells S, Ferrari P, Gaetz W, Bostan AC (2008): Self-paced movements induce high-frequency gamma oscillations in primary motor cortex. NeuroImage 42:332–342.

Chiarenza GA, Villa M, Vasile G (1995): Developmental aspects of bereitschaftspotential in children during goal-directed behaviour. Int J Psychophysiol 19:149–176.

Chisholm RC, Karrer R (1988): Movement-related potentials and control of associated movements. Int J Neurosci 42:131–148.

Dayanidhi S, Hedberg A, Valero-Cuevas FJ, Forssberg H (2013): Developmental improvements in dynamic control of fingertip forces last throughout childhood and into adolescence. J Neurophysiol 110:1583–1592.

Engel AK, Fries P (2010): Beta-band oscillations—Signalling the status quo? Curr Opin Neurobiol 20:156–165.

Erdler M, Beisteiner R, Mayer D, Kaindl T, Edward V, Windischberger C, Lindinger G, Deecke L (2000): Supplementary motor area activation preceding voluntary movement is detectable with a whole-scalp magnetoencephalography system. NeuroImage 11:697–707.

Fonov V, Evans AC, Botteron K, Almli CR, McKinstry RC, Collins DL (2011): Unbiased average age-appropriate atlases for pediatric studies. NeuroImage 54:313–327.

Forssberg H, Eliasson AC, Kinoshita H, Johansson RS, Westling G (1991): Development of human precision grip I: Basic coordination of force. Exp Brain Res 85:451–457.

Gaetz W, Macdonald M, Cheyne D, Snead OC (2010): Neuromagnetic imaging of movement-related cortical oscillations in children and adults: Age predicts post-movement beta rebound. NeuroImage 51:792–807.

Gaetz W, Edgar JC, Wang DJ, Roberts TP (2011): Relating MEG measured motor cortical oscillations to resting gamma-aminobutyric acid (GABA) concentration. NeuroImage 55:616–621.

Giedd JN, Blumenthal J, Jeffries NO, Castellanos FX, Liu H, Zijdenbos A, Paus T, Evans AC, Rapoport JL (1999): Brain development during childhood and adolescence: A longitudinal MRI study. Nat Neurosci 2:861–863.

Grezes J, Decety J (2001): Functional anatomy of execution, mental simulation, observation, and verb generation of actions: A meta-analysis. Hum Brain Mapp 12:1–19.

Heinen F, Glocker FX, Fietzek U, Meyer BU, Lucking CH, Korinthenberg R (1998): Absence of transcallosal inhibition following focal magnetic stimulation in preschool children. Ann Neurol 43:608–612.

Herdman AT, Ryan JD (2007): Spatio-temporal brain dynamics underlying saccade execution, suppression, and error-related feedback. J Cogn Neurosci 19:420–432.

Holmes CJ, Hoge R, Collins L, Woods R, Toga AW, Evans AC (1998): Enhancement of MR images using registration for signal averaging. J Comput Assist Tomogr 22:324–333.

Huo X, Wang Y, Kotecha R, Kirtman EG, Fujiwara H, Hemasilpin N, Degrauw T, Rose DF, Xiang J (2011): High gamma oscillations of sensorimotor cortex during unilateral movement in the developing brain: A MEG study. Brain Topogr 23:375–384.

Huttenlocher PR (1979): Synaptic density in human frontal cortex—Developmental changes and effects of aging. Brain Res 163:195–205.

Jenkinson N, Brown P (2011): New insights into the relationship between dopamine, beta oscillations and motor function. Trends Neurosci 34:611–618.

Jenkinson M, Beckmann CF, Behrens TE, Woolrich MW, Smith SM (2012): Fsl. NeuroImage 62:782–790.

Johnson BW, Crain S, Thornton R, Tesan G, Reid M (2010): Measurement of brain function in pre-school children using a custom sized whole-head MEG sensor array. Clin Neurophysiol 121:340–349.

Johnson BW, McArthur G, Hautus M, Reid M, Brock J, Castles A, Crain S (2013): Lateralized auditory brain function in children with normal reading ability and in children with dyslexia. Neuropsychologia 51:633–641.

Jokisch D, Daum I, Suchan B, Troje NF (2005): Structural encoding and recognition of biological motion: evidence from event-related potentials and source analysis. Behav Brain Res 157: 195–204.

Jones SR, Pritchett DL, Sikora MA, Stufflebeam SM, Hamalainen M, Moore CI (2009): Quantitative analysis and biophysically realistic neural modeling of the MEG mu rhythm: Rhythmogenesis and modulation of sensory-evoked responses. J Neurophysiol 102:3554–3572.

Jones SR, Kerr CE, Wan Q, Pritchett DL, Hamalainen M, Moore CI (2010): Cued spatial attention drives functionally relevant modulation of the mu rhythm in primary somatosensory cortex. J Neurosci 30:13760–13765.

Jurkiewicz MT, Gaetz WC, Bostan AC, Cheyne D (2006): Post-movement beta rebound is generated in motor cortex: Evidence from neuromagnetic recordings. Neuroimage 32:1281–1289.

Kornhuber HH, Deecke L (1965): [Changes in the Brain Potential in Voluntary Movements and Passive Movements in Man: Readiness Potential and Reafferent Potentials]. Pflugers Arch Gesamte Physiol Menschen Tiere 284:1–17.

Kristeva R, Cheyne D, Deecke L (1991): Neuromagnetic fields accompanying unilateral and bilateral voluntary movements: Topography and analysis of cortical sources. Electroencephalogr Clin Neurophysiol 81:284–298.

Lalancette M, Quraan M, Cheyne D (2011): Evaluation of multiple-sphere head models for MEG source localization. Phys Med Biol 56:5621–5635.

Lalo E, Thobois S, Sharott A, Polo G, Mertens P, Pogosyan A, Brown P (2008): Patterns of bidirectional communication between cortex and basal ganglia during movement in patients with Parkinson disease. J Neurosci 28:3008–3016.

Lancaster JL, Woldorff MG, Parsons LM, Liotti M, Freitas CS, Rainey L, Kochunov PV, Nickerson D, Mikiten SA, Fox PT (2000): Automated Talairach atlas labels for functional brain mapping. Hum Brain Mapp 10:120–131.

Lauronen L, Nevalainen P, Wikstrom H, Parkkonen L, Okada Y, Pihko E (2006): Immaturity of somatosensory cortical processing in human newborns. NeuroImage 33:195–203.

Lippe S, Martinez-Montes E, Arcand C, Lassonde M (2009): Electrophysiological study of auditory development. Neuroscience 164:1108–1118.

Litvak V, Eusebio A, Jha A, Oostenveld R, Barnes GR, Penny WD, Zrinzo L, Hariz MI, Limousin P, Friston KJ, Brown P (2010): Optimized beamforming for simultaneous MEG and intracranial local field potential recordings in deep brain stimulation patients. NeuroImage 50:1578–1588.

Litvak V, Mattout J, Kiebel S, Phillips C, Henson R, Kilner J, Barnes G, Oostenveld R, Daunizeau J, Flandin G, Penny W, Friston K (2011): EEG and MEG data analysis in SPM8. Comput Intell Neurosci 2011:852961.

Makeig S, Delorme A, Westerfield M, Jung TP, Townsend J, Courchesne E, Sejnowski TJ (2004): Electroencephalographic brain dynamics following manually responded visual targets. PLoS Biol 2:e176.

Marshall PJ, Young T, Meltzoff AN (2011): Neural correlates of action observation and execution in 14-month-old infants: An event-related EEG desynchronization study. Dev Sci 14:474–480.

Mayston MJ, Harrison LM, Stephens JA (1999): A neurophysiological study of mirror movements in adults and children. Ann Neurol 45:583–594.

Moore JK, Guan YL (2001): Cytoarchitectural and axonal maturation in human auditory cortex. J Assoc Res Otolaryngol 2:297–311.

Muller K, Homberg V, Lenard HG (1991): Magnetic stimulation of motor cortex and nerve roots in children. Maturation of cortico-motoneuronal projections. Electroencephalogr Clin Neurophysiol 81:63–70.

Muthukumaraswamy SD (2010): Functional properties of human primary motor cortex gamma oscillations. J Neurophysiol 104: 2873–2885.

Muthukumaraswamy SD, Edden RA, Jones DK, Swettenham JB, Singh KD (2009): Resting GABA concentration predicts peak

gamma frequency and fMRI amplitude in response to visual stimulation in humans. Proc Natl Acad Sci USA 106:8356–8361.
Nagamine T, Kajola M, Salmelin R, Shibasaki H, Hari R (1996): Movement-related slow cortical magnetic fields and changes of spontaneous MEG- and EEG-brain rhythms. Electroencephalogr Clin Neurophysiol 99:274–286.
Nezu A, Kimura S, Uehara S, Kobayashi T, Tanaka M, Saito K (1997): Magnetic stimulation of motor cortex in children: Maturity of corticospinal pathway and problem of clinical application. Brain Dev 19:176–180.
Oldfield RC (1971): The assessment and analysis of handedness: The Edinburgh inventory. Neuropsychologia 9:97–113.
Onishi H, Soma T, Kameyama S, Oishi M, Fuijmoto A, Oyama M, Furusawa AA, Kurokawa Y (2006): Cortical neuromagnetic activation accompanying two types of voluntary finger extension. Brain Res 1123:112–118.
Pfurtscheller G, Aranibar A (1977): Event-related cortical desynchronization detected by power measurements of scalp EEG. Electroencephalogr Clin Neurophysiol 42:817–826.
Pfurtscheller G, Stancak A Jr, Neuper C (1996): Event-related synchronization (ERS) in the alpha band—An electrophysiological correlate of cortical idling: A review. Int J Psychophysiol 24: 39–46.
Picton TW, Taylor MJ (2007): Electrophysiological evaluation of human brain development. Dev Neuropsychol 31:249–278.
Piek JP, Hands B, Licari MK (2012): Assessment of motor functioning in the preschool period. Neuropsychol Rev 22:402–413.
Pihko E, Nevalainen P, Stephen J, Okada Y, Lauronen L (2009): Maturation of somatosensory cortical processing from birth to adulthood revealed by magnetoencephalography. Clin Neurophysiol 120:1552–1561.
Ponton CW, Eggermont JJ, Kwong B, Don M (2000): Maturation of human central auditory system activity: Evidence from multichannel evoked potentials. Clin Neurophysiol 111:220–236.
Ponton C, Eggermont JJ, Khosla D, Kwong B, Don M (2002): Maturation of human central auditory system activity: Separating auditory evoked potentials by dipole source modeling. Clin Neurophysiol 113:407–420.
Rajapakse T, Kirton A (2013): Non-invasive brain stimulation in children: Applications and future directions. Transl Neurosci 4:217–233.
Robinson SE, Vrba J (1999): Functional Neuroimaging by Synthetic Aperture Magnetometry. Sendai: Tohoku University Press.
Rorden C, Brett M (2000): Stereotaxic display of brain lesions. Behav Neurol 12:191–200.
Salmelin R, Hari R (1994): Spatiotemporal characteristics of sensorimotor neuromagnetic rhythms related to thumb movement. Neuroscience 60:537–550.
Sarvas J (1987): Basic mathematical and electromagnetic concepts of the biomagnetic inverse problem. Phys Med Biol 32:11–22.
Singh KD, Barnes GR, Hillebrand A (2003): Group imaging of task-related changes in cortical synchronisation using nonparametric permutation testing. Neuroimage 19:1589–1601.
Southgate V, Johnson MH, Osborne T, Csibra G (2009): Predictive motor activation during action observation in human infants. Biol Lett 5:769–772.
Tallon-Baudry C, Bertrand O, Delpuech C, Pernier J (1997): Oscillatory gamma-band (30–70 Hz) activity induced by a visual search task in humans. J Neurosci 17:722–734.
Tesan G, Johnson BW, Reid M, Thornton R, Crain S (2010): Measurement of neuromagnetic brain function in pre-school children with custom sized MEG. J Vis Exp 36:1693.
Tucker DM (1993): Spatial sampling of head electrical fields: the geodesic sensor net. Electroencephalogr Clin Neurophysiol 87: 154–163.
Wehner DT, Hamalainen MS, Mody M, Ahlfors SP (2008): Head movements of children in MEG: Quantification, effects on source estimation, and compensation. NeuroImage, 40:541–550.
Wilson TW, Slason E, Asherin R, Kronberg E, Reite ML, Teale PD, Rojas DC (2010): An extended motor network generates beta and gamma oscillatory perturbations during development. Brain Cogn 73:75–84.